Research Square

Preprints are preliminary reports that have not undergone peer review.
They should not be considered conclusive, used to inform clinical practice,
or referenced by the media as validated information.

Efficacy of Nano-Formulated Nitazoxanide Compared to Bulk Powder Against Human Oral Squamous Cell Carcinoma Cell line

Moataz Mohamed Elkholy
October University for Modern Sciences and Arts
Mohamed Sobhy Kishta
National Research Centre
Beshoy Magdy M Moharib
October University for Modern Sciences and Arts
Sara Mohamed Ali
smaly@msa.edu.eg

October University for Modern Sciences and Arts

Article

Keywords: Drug repurposing, Nitazoxanide, Oral squamous cell carcinoma, nanomedicine.

Posted Date: July 6th, 2026

DOI: https://doi.org/10.21203/rs.3.rs-10073017/v1

License: This work is licensed under a Creative Commons Attribution 4.0 International License.
Read Full License

Additional Declarations: No competing interests reported.

Abstract

Purpose

Oral Squamous Cell Carcinoma (OSCC) represents approximately 90% of all oral malignancies. Limitations in current chemotherapy necessitates the exploration of repurposed drugs and novel delivery systems. Nitazoxanide drug (NTZ) has long been used for the treatment for parasitic infections, It was proven to have a promising anti-cancer activity for colorectal cancer. While powdered NTZ is proven effective *in vitro*, its clinical application is limited by poor aqueous solubility and low bioavailability as nano-formulation offers enhanced solubility by increasing the surface area for drug-cell interaction, targeted delivery to accumulate drug concentrations within the tumor microenvironment and reduced IC50. The present study aims to evaluate and compare the anticancer effects of powdered and nano-formulated Nitazoxanide (NTZ-NS) against oral cancer cell line.

Methods

We utilized SCC-9 cell line as cancer model, and HaCaT keratinocytes as non-malignant controls. Cells were assigned into the four experimental groups: positive controls, negative controls, NTZ free drug treated, NTZ nanoparticles treated. Each treatment were tested across multiple concentrations for 24–72 h. Cell viability were assessed using the MTT assay to generate dose–response curves and IC_{50} values. Cell-cycle, Apoptosis and quantified BCL2 and VEGF proteins by ELISA were performed.

Results

MTT analysis showed a dose-dependent cytotoxicity of NTZ in SCC-9 cells, with minimal effects on HaCaT normal cells. Cell cycle analysis showed that treatment with free NTZ significantly increased the subG1 population to 15.0%, with notable S-phase (12%) and G2/M (6.2%) accumulation, indicating induction of apoptosis and cell-cycle arrest. NTZ-NS further enhanced subG1 accumulation to 19%, while drastically reducing S (0.7%) and G2/M (0.2%) phases, Flow cytometric analysis of apoptosis revealed that treatment with free NTZ significantly increased late apoptosis (32.3%) and necrosis (5.2%), reducing viable cells to 60.6%. Notably, NTZ-NS induced a more pronounced effect, with late apoptosis reaching 45.4%, necrosis 11.0%, and viable cells decreasing to 42.9%, demonstrating enhanced apoptotic induction compared to the free drug. Treatment with free NTZ significantly reduced BCL-2 and VEGF expression, while NTZ-NS induced a more pronounced suppression, restoring marker levels toward those observed in normal cells.

Conclusion

These findings indicate that NTZ exerts anticancer effects through induction of apoptosis and inhibition of angiogenic signaling, with nanoformulation markedly enhancing its biological efficacy.

Introduction

Oral squamous cell carcinoma (OSCC) represents the vast majority of approximately 90% of all oral cavity malignancies [1]. Recent epidemiological data from 2024 documented approximately 58,450 incident cases and 12,230 fatalities worldwide, underscoring an escalating burden. This is further evidenced by a 113.9% increase in global mortality rate since 1990, with lip and oral cavity cancers (LOCC) reaching 208,379 deaths annually by 2021 [2]. OSCC is characterized by aggressive clinical behavior and high tendency for cervical lymph node metastasis. OSCC traditional risk factors include smoking, smokeless tobacco, and heavy alcohol consumption[3]. Despite advancements in multidisciplinary therapeutic strategies, including surgical resection, radiotherapy, and immunotherapy, the five-year survival rate for OSCC has remained largely stagnant at roughly 50–60% over the past several decades [1,3].

Traditional treatment modalities for oral squamous cell carcinoma (OSCC) are frequently undermined by many clinical side effects and systemic toxicities. While surgery remains the definitive primary treatment option, it often results in functional impairment, aesthetic disfigurement, and psychological despair, particularly in advanced cases[1]. Furthermore, definitive radiotherapy and chemotherapy are constrained by a narrow therapeutic index, leading to severe adverse events such as osteoradionecrosis, debilitating mucositis, and cumulative nephrotoxicity, alongside the persistent challenge of multidrug resistance (MDR) and locoregional recurrence[1,3]. In response to these restrictions, the repurposing of FDA-approved anti-parasitic drugs has emerged as a promising alternative, utilizing their established safety profiles and cost-effectiveness. Drug repurposing is discovering new biological targets for existing drugs that have already been approved for the treatment of other diseases. Recent evidence highlights the potent anti-tumor activity of anti-parasitic agents in inhibiting cancer stem-like cells[4].

Nitazoxanide (NTZ) is a broad-spectrum antiparasitic agent that has a wide-spectrum antimicrobial effect against viruses, anaerobic bacteria, helminths and protozoa[5]. NTZ traditionally utilized as an FDA-approved antiprotozoal and antiviral agent, has recently gained significant attention as a potential candidate for drug repurposing in cancer therapy. Its antineoplastic efficacy is primarily driven by its ability to modulate critical oncogenic signaling pathways that are typically dysregulated in head and neck malignancies. Emerging evidence from 2025 demonstrates that NTZ exerts a potent inhibitory effect on OSCC progression by targeting the Wnt/β-catenin and c-Myc axes, which are central to tumor cell proliferation, survival, and the maintenance of cancer stemness[6,7]. Furthermore, innovative spatial transcriptomic analyses have revealed that NTZ can suppress the development of head and neck squamous cell carcinoma (HNSCC) by regulating autophagy-related hub genes, such as BIRC5 and CDKN2A, thereby overcoming the metabolic adaptations that often lead to conventional chemoresistance[7]. Additionally, NTZ has been identified as a selective oxidative phosphorylation

(OXPHOS) inhibitor, which allows it to specifically target the quiescent, glucose-deprived tumor cell populations that frequently survive traditional radiotherapy and cause locoregional recurrence[7]. These multifaceted mechanisms, combined with its established safety profile and low systemic toxicity, position nitazoxanide as a promising and cost-effective alternative to traditional, more debilitating treatment modalities for OSCC.

Aim of the study:

Evaluation and comparison of the anticancer effects of powdered and nano-formulated against oral cancer cell line. Findings from this research will help in proving the anticancer effect against oral squamous cell carcinoma.

Materials and Methods

Study Design

This in vitro experimental study was designed to evaluate and compare the anticancer efficacy and cellular effects of free nitazoxanide (NTZ) and its nanoformulation (NTZ-NS) on oral squamous cell carcinoma (OSCC) and normal epithelial cell models. Human SCC-9 cells were used as the OSCC model (positive control for malignancy), while HaCaT keratinocytes served as the non-malignant epithelial control (negative control). SCC-9 and HaCaT cell lines were both purchased from VACSERA (The Holding Company for Biological Products and Vaccines), Giza, Egypt. Cells were cultured under standard conditions and randomly allocated into experimental groups for each cell line as follows: (i) **negative control group**, consisting of untreated HaCaT cells; (ii) **positive control group**, consisting of untreated SCC-9 cells; (iii) **treated group 1**, SCC-9 cells treated with free NTZ at the IC_{50} concentration determined by MTT assay; and (iv) **treated group 2**, SCC-9 cells treated with nano-nitazoxanide (NTZ-NS) at the corresponding IC_{50}-equivalent concentration. All treatments were incubated for 24 h to capture early apoptotic and cell-cycle responses based on literature-supported optimization for epithelial cancer cells.

Each experimental condition was performed in triplicate and repeated in three independent biological experiments to ensure reproducibility and statistical reliability. Following treatment, cells were analyzed using metabolic viability assessment (MTT assay), apoptotic pathway evaluation via ELISA quantification of Human BCL2 and cell-cycle regulation via Human VEGF ELISA kits, along with flow cytometric analysis of apoptosis and cell-cycle distribution. This design enabled systematic comparison of free versus nanoformulated NTZ in terms of cytotoxic potency, selective targeting of malignant cells, induction of apoptosis, and disruption of cell-cycle progression, thereby providing functional validation of NTZ's anticancer efficacy.

Preparation of Nitazoxanide Nanoparticles (NTZ-NS)

Nitazoxanide nanoparticles (NTZ-NS) were prepared using a modified nanoemulsion solvent-evaporation technique to achieve a uniform particle size in the nanoscale range (40–80 nm). Briefly, NTZ (10 mg) was dissolved in 2 mL of acetone as the organic phase, and a lipid component (e.g., lecithin or DSPE-PEG, 20 mg) was added to enhance encapsulation and stability. The organic solution was slowly injected into 10 mL of aqueous phase containing 1% (w/v) Tween 80 under constant magnetic stirring at 800 rpm at room temperature. The resulting emulsion was sonicated for 10 min using a probe sonicator at 40% amplitude in pulse mode (5 s on/5 s off) to reduce droplet size and achieve homogeneity. The organic solvent was then removed under reduced pressure using a rotary evaporator at 40°C, yielding a stable NTZ nano-suspension. The nanoparticle dispersion was further filtered through a 0.22 µm membrane to remove aggregates and stored at 4°C until further use. Particle size and morphology were characterized by transmission electron microscope (TEM) and dynamic light scattering (DLS) to ensure uniformity, while zeta potential measurements were conducted to confirm colloidal stability. The final NTZ-NS formulation exhibited enhanced aqueous dispersibility, uniform nanoscale size, and potential for improved cellular uptake, making it suitable for in vitro anticancer studies [8–11].

Characterization of NTZ Nanoparticles

Particle size, polydispersity index (PDI), and zeta potential were determined by DLS in which the average diameter, the size distribution, and zeta potential of samples were measured by using a particle size analyzer (Nano-ZS, Malvern Instruments Ltd., UK). For measuring Size distribution and zeta potential, the sample was sonicated for 10–20 min. just before assessment. The morphology was confirmed by TEM which was connected to a CCD camera at an accelerating voltage of 200 kV, was used to analyze the size and shape of nanoparticles (NPs). On a thin layer of amorphous carbon that had been deposited on a copper grid (300 mesh), one drop of the NPs was placed. After allowing the solution to air dry, the sample was inspected under a microscope or measured for nanoparticles using micrographs[10,12].

Cell Viability Assessment (MTT Assay)

Cell viability following treatment with free NTZ or NTZ -NS were evaluated using the MTT assay. Treated and control cells were incubated with MTT reagent, and the resulting formazan crystals were solubilized and quantified spectrophotometrically. Dose–response curves were measured, and IC_{50} values were calculated to compare the cytotoxic potency of free versus NTZ -NS across cancerous and non-cancerous cell lines. Cells were treated with free NTZ or NTZ -NS at concentrations of **0.5, 1, 2, 5, 10, 20 and 40 µM**, which correspond to reported anticancer concentrations of NTZ in epithelial cancers. Absorbance was measured at 570 nm, and cell viability percentages were calculated relative to untreated controls.

Flow Cytometric Analysis of Apoptosis and Cell Cycle

Apoptosis and cell-cycle progression were quantitatively analyzed by flow cytometry following treatment with free NTZ or NTZ -NS at their respective IC_{50} concentrations. Cells were collected by trypsinization, washed twice with ice-cold phosphate-buffered saline (PBS), and counted using a hemocytometer to ensure uniform cell density across samples. For apoptosis analysis, approximately 1 × 10^6 cells were resuspended in 100 µL of 1× Annexin V binding buffer and stained with Annexin V–FITC (5 µL) and propidium iodide (PI, 5 µL) using a commercial apoptosis detection kit, followed by incubation for 15 min at room temperature in the dark. After incubation, 400 µL of binding buffer was added, and samples were immediately analyzed by flow cytometry, enabling discrimination of viable (Annexin V^-/PI^-), early apoptotic (Annexin V^+/PI^-), late apoptotic (Annexin V^+/PI^+), and necrotic (Annexin V^-/PI^+) populations.

For cell-cycle analysis, a separate aliquot of treated and control cells was fixed dropwise in 70% ice-cold ethanol while vortexing gently to prevent cell clumping, followed by incubation at – 20°C for a minimum of 12–24 h to ensure complete fixation and membrane permeabilization. Fixed cells were then centrifuged, washed twice with PBS to remove residual ethanol, and resuspended in PBS containing RNase A (100 µg/mL) for 30 min at 37°C to degrade RNA and prevent interference with DNA staining. Subsequently, cells were stained with propidium iodide (PI, 50 µg/mL) for 30 min at room temperature in the dark. DNA content was analyzed using a flow cytometer equipped with a 488 nm argon laser, and at least 10,000–20,000 events per sample were acquired. Doublets and aggregates were excluded using forward scatter–area versus forward scatter–height (FSC-A/FSC-H) gating. Cell-cycle distribution was quantified using DNA content histograms and mathematical modeling to determine the percentages of cells in subG1 (apoptotic fraction), G0/G1, S, and G2/M phases. Data analysis was performed using dedicated flow cytometry software, enabling accurate assessment of cell-cycle arrest, apoptotic DNA fragmentation, and treatment-induced cell-cycle perturbations across control, free-drug, and nanoformulation-treated groups.

Quantification of ELISA Markers

Protein levels of Human Bcl-2 ELISA Kit (E-EL-H0114), Human VEGF-A (Vascular Endothelial Cell Growth Factor A) ELISA Kit (E-EL-H0111) were quantified using ELISA kits. Culture supernatants were collected after treatment, and absorbance values were measured according to manufacturer instructions.

Results

Nanoparticle Characterization

TEM revealed that nitazoxanide nanoparticles were well-formed and spherical, with mean particle diameters of **64.67 nm, 45.35 nm, and 53.86 nm** across multiple fields, indicating a relatively narrow size distribution. DLS measurements showed a closely matching hydrodynamic size, confirming the nanoscale dimensions and uniformity of the formulation. These data indicate that the NTZ-NS formulation is stable, monodispersed, and suitable for cellular uptake studies (Fig. 1).

(A and B) TEM micrographs showing spherical, well-dispersed NTZ nanoparticles with diameters of 64.67 nm, 45.35 nm, and 53.86 nm. (C) DLS size distribution profile confirming a hydrodynamic diameter consistent with TEM measurements, indicating uniform nanoparticle size and stable dispersion

MTT Assay for NTZ and NTZ-NS

MTT analysis showed a dose-dependent cytotoxicity of NTZ in SCC-9 cells, with minimal effects on HaCaT normal cells. Cell viability of untreated SCC-9 cells was near 100%, while treatment with free NTZ reduced viability to 68% at 2 μM, 52% at 5 μM, and 38% at 10 μM. NTZ-NS further enhanced cytotoxicity, lowering SCC-9 viability to 52% at 2 μM, 38% at 5 μM, and 25% at 10 μM. HaCaT cells maintained > 90% viability across all concentrations (0.5–40 μM), indicating selective cytotoxicity toward cancer cells (Fig. 2). Nonlinear regression analysis of the SCC-9 viability data yielded IC_{50} values of ~ 2.1 μM for free NTZ and ~ 1.5 μM for NTZ-NS. Based on these IC_{50} values and cytotoxicity trends, 2 μM NTZ and 1.5 μM NTZ-NS were selected for all subsequent apoptosis, cell-cycle, and ELISA experiments, ensuring effective anticancer activity while minimizing effects on normal epithelial cells.

Apoptosis Analysis for NTZ and NTZ-NS

Flow cytometric analysis of apoptosis revealed that untreated HaCaT cells (negative control) maintained high viability (93.0%), with minimal early (0.5%) and late (3.7%) apoptosis, and low necrosis (1.9%). Untreated SCC-9 cells (positive control) also showed high viability (94.1%), indicating intrinsic resistance to apoptosis. Treatment with free NTZ significantly increased late apoptosis (32.3%) and necrosis (5.2%), reducing viable cells to 60.6%. Notably, NTZ-NS induced a more pronounced effect, with late apoptosis reaching 45.4%, necrosis 11.0%, and viable cells decreasing to 42.9%, demonstrating enhanced apoptotic induction compared to the free drug (Fig. 3).

Cell-Cycle Analysis for NTZ and NTZ-NS

Flow cytometric analysis of cell-cycle distribution showed that untreated HaCaT cells (negative control) were predominantly in the G0/G1 phase (96.3%) with minimal subG1 (1.9%), S (0.2%), and G2/M (0.1%) populations. Untreated SCC-9 cells (positive control) exhibited a similar profile, confirming normal proliferation and resistance to spontaneous apoptosis. Treatment with free NTZ significantly increased the subG1 population to 15.0%, with notable S-phase (12%) and G2/M (6.2%) accumulation, indicating induction of apoptosis and cell-cycle arrest. NTZ-NS further enhanced subG1 accumulation to 19%, while drastically reducing S (0.7%) and G2/M (0.2%) phases, suggesting strong apoptosis induction and effective disruption of cell-cycle progression in SCC-9 cells (Fig. 4).

ELISA Analysis for NTZ and NTZ-NS

NTZ treatment significantly modulated apoptosis and angiogenesis related biomarkers in SCC-9 oral squamous cell carcinoma cells. ELISA analysis revealed a marked elevation of BCL-2 and VEGF levels in untreated SCC-9 cells compared with HaCaT normal keratinocytes, confirming the anti-apoptotic and

pro-angiogenic phenotype of OSCC cells. Treatment with free NTZ significantly reduced BCL-2 and VEGF expression, while NTZ-NS induced a more pronounced suppression, restoring marker levels toward those observed in normal cells (Fig. 5). These findings indicate that NTZ exerts anticancer effects through induction of apoptosis and inhibition of angiogenic signaling, with nanoformulation markedly enhancing its biological efficacy.

All experimental data were expressed as the mean ± standard deviation (SD) from at least three independent biological experiments, each performed in triplicate to ensure reproducibility. Statistical comparisons between the experimental groups including untreated controls, free-drug treated, and nanoformulation-treated groups were performed using one-way analysis of variance (ANOVA), followed by post-hoc test to identify significant differences between specific pairs. For cell viability assays, IC_{50} values were determined through non-linear regression analysis of the dose-response curves. *: significant difference between HaCaT and SCC-9 ($p < 0.05$), #: significant difference between SCC-9 (NTZ) and SCC-9 ($p < 0.01$), and &: significant difference between SCC-9 (NTZ-NS) and SCC-9 ($p < 0.01$), @: significant differences between SCC-9 (NTZ) and SCC-9 (NTZ -NS) ($p < 0.05$). Statistical analyses and graphing were conducted using GraphPad Prism version 8.0.

Discussion

OSCC management remains a constant challenge, primarily due to the high mortality rates and the side effects associated with conventional treatment modalities. Our study demonstrates that NTZ an FDA-approved antiparasitic, can successfully be repurposed as an anticancer agent against SCC-9 cell line. Furthermore, the transition from bulk powder to a nano-formulated form significantly enhances its therapeutic potential, proved by reduced cell viability, increased apoptosis, and more effective cell-cycle arrest.

In our study MTT analysis showed a dose-dependent cytotoxicity of NTZ in SCC-9 cells, with minimal effects on HaCaT normal cells and enhanced effect of NTZ-Ns ensuring effective anticancer activity while minimizing effects on normal epithelial cells, these results were consistent with Yang et al. 2024 results which indicated that NTZ had the time and concentration dependent ability to inhibit the proliferation of epithelial ovarian cancer cells[13].

These results are explained by the ability of NTZ to modulate complex oncogenic signaling pathways including Wnt/β-catenin signaling pathway which is a major promotor of cell proliferation in OSCC where β-catenin accumulation provokes its translocation into the nucleus activating growth-promoting genes[6]. NTZ disrupts this pathway by stimulating Glycogen Synthase Kinase-3β (GSK-3β), which targets β-catenin phosphorylation and their subsequent degradation[14]. Since C-Myc and Cyclin D1 are direct downstream targets of the β-catenin/TCF4 transcriptional complex, its expression levels drop significantly following NTZ treatment promoting antitumor effect [13].

In the current study, the flow cytometric analysis of apoptosis revealed that treatment with free NTZ significantly reduced viable cells to 60.6% while NTZ-NS induced a more pronounced apoptotic effect, with viable cells decreasing to 42.9%, demonstrating enhanced apoptotic induction compared to the free drug, whereas the negative and positive control groups maintained high viability. These results were consistent with[15] Di Santo and Ehrisman, 2013 who stated that NTZ treatment also proved a pro-apoptotic effect through downregulation of the anti-apoptotic protein BCL-2 and the subsequent activation of caspase-dependent intrinsic pathway of apoptosis Abd El-Fadeal et al., 2021 proved that NTZ significantly increased early, intermediate, and late apoptotic cell death of colon cancer cell line[14]. and Lu et al., 2022 who suggested that NTZ may also target the 20S proteasome, preventing the degradation of pro-apoptotic regulators and leading to cell cycle arrest[16].

Our results proved that NTZ treatment led to effective disruption of cell-cycle progression in SCC-9 cells with significant increase of the NTZ treated cell subG1population to 15.0%, with notable S-phase (12%) and G2/M (6.2%) accumulation, indicating induction of apoptosis and cell-cycle arrest, with further enhanced of NTZ-NS treated cells with subG1 accumulation to 19%, while drastically reducing S (0.7%) and G2/M (0.2%) phases. These results are in harmony with the results of Abd El-Fadeal et al., 2021, who stated that NTZ treatment prompted the cell cycle arrest of the pre-G1 and G2/M-phases in colon cancer cell line[14]. According to, Other studies also showed that NTZ treatment induced G1/G0 phase and G1 phase cell cycle arrest in of colorectal cancer and anaplastic thyroid cancer cell lines[17,18] .

These results could be attributed to mitochondrial function disruption, disrupting oxidative phosphorylation that will lead to metabolic stress causing mTOR/c-Myc pathway inhibition promoting apoptosis, NTZ also causes p27 stabilization which prevents the transition from G1 to S phase [17]. As NTZ has been identified as an inhibitor of the 20S proteasome, which is critical for cell cycle regulators degradation as cyclins. NTZ helps moderate inhibitor of the STAT3 signaling pathway. Since STAT3 regulates the transcription of various genes essential for cell cycle progression as Cyclin D1, its suppression by NTZ contributes to the overall anti-proliferative effect in multiple cancer cell lines[16].

The anti-tumor efficacy of NTZ was also proved by our results of downregulation of BCL2 and VEGF These effects are primarily mediated through the inhibition of the STAT3 and Wnt/β-catenin signaling pathways. As STAT3 is a primary transcription factor for BCL2 and VEGF. NTZ inhibits the phosphorylation and nuclear translocation of STAT3, leading to silencing of the transcription of these survival and angiogenic genes[16]. BCL2 downregulation will facilitatie the release of Cytochrome c and subsequent activation of the caspase cascade[19] .

Since NTZ has been characterized as an inhibitor of Wnt/β-catenin signaling, which is frequently stimulated in solid tumors. β-catenin directly regulates VEGF expression in the tumor microenvironment. By promoting the degradation of β-catenin or inhibiting its transcriptional activity, NTZ indirectly leads to a significant reduction in VEGF secretion, thereby impairing tumor angiogenesis[20–22].

The enhanced effect of NTZ-NS over bulk powder is likely due to the increased surface area-to-volume ratio of the nanoparticles (40–80 nm), which improves aqueous solubility and bioavailability. The enhanced permeability and retention (EPR) effect allows for better drug accumulation within the tumor microenvironment. This resulted in a significantly lower IC_{50} for NTZ-NS of 1.5 μM compared to free NTZ of 2.1 μM, and a more pronounced accumulation of cells in the subG1 phase with 19% versus 15.0%, indicating more efficient DNA fragmentation and apoptosis. While someprevious studies on powdered NTZ suggested limited clinical application due to poor solubility, our study addresses this through nanotechnology.

Conclusion

The integration of nanotechnology with drug repurposing offers a promising treatment modality for OSCC treatment. By enhancing the delivery of a drug with a well-established safety profile like nitazoxanide, we can achieve high selective toxicity against malignant cells while sparing healthy tissue.

Declarations

We confirm that this manuscript is original, has not been published elsewhere, and is not currently under consideration by another journal and that all authors have read and approved the manuscript and agree with its submission to Head and Neck Pathology.

Statistical methods employed are performed by Dr. Mohamed Sobhy Kishta, with authorship on the manuscript.

Consent to publication: All authors gave their consent to publish this work**.**

Ethical committee approval: Not applicable.

Competing interest: The authors have no competing interests to report.

Author's contribution: M.M.E., M.S.K., B.M.M. and S.M.A. contributed equally to this research article.

Funding: This research article didn't receive any funding.

Data availability: All data generated or analysed during this study are included in this published article.

Acknowledgements: Not applicable.

Author Contribution

M. El-Kholy helped in formulating the study idea, data collection, data analysis, data interpretation, manuscript revisionM. S. Kishta Performed the experiment and its data collectionB. M. Moharib helped

in formulating the study idea and data collection.S. M. Ali helped in formulating the study idea, data collection, data analysis, data interpretation, manuscript writing

References

1. Mohamad, I. et al. Current Treatment Strategies and Risk Stratification for Oral Carcinoma. *Am. Soc. Clin. Oncol. Educational Book.* (43). 10.1200/EDBK_389810 (2023).
2. Meng, S., Lv, A., Li, N. & Ding, X. Global, regional, and national burden of lip and oral cavity cancer and projections to 2036. *BMC Cancer*. **25** (1), 1573. 10.1186/s12885-025-14995-z (2025).
3. Fatima, J. et al. Comprehensive Analysis of Oral Squamous Cell Carcinomas: Clinical, Epidemiological, and Histopathological Insights With a Focus on Prognostic Factors and Survival Time. *Cureus Published online Febr.* **18** 10.7759/cureus.54394 (2024).
4. Tantawy, R., Raafat, S. N., El-Gawish, A. & Ghalwash, D. Synergistic potential of Ivermectin and doxorubicin in oral squamous cell carcinoma: an in vitro investigation. *BMC Pharmacol. Toxicol.* **27** (1), 16. 10.1186/s40360-025-01053-4 (2025).
5. Hassan, A. M. et al. Efficacy and safety of nitazoxanide based quadruple regimen as first line therapy for treating Helicobacter pylori infected naïve patients. *J. Infect. Developing Ctries.* **19** (06), 843–849. 10.3855/jidc.20505 (2025).
6. Reyes, M., Flores, T., Betancur, D., Peña-Oyarzún, D. & Torres, V. A. Wnt/β-Catenin Signaling in Oral Carcinogenesis. *Int. J. Mol. Sci.* **21** (13), 4682. 10.3390/ijms21134682 (2020).
7. Jiang, X. et al. Integrating single-cell RNA sequencing and spatial transcriptomics reveals the therapeutic effect of nitazoxanide in head and neck squamous cell carcinoma. *Discover Oncol.* **16** (1), 1509. 10.1007/s12672-025-03372-8 (2025).
8. Muniswamy, V. J. et al. Dendrimer-Cationized-Albumin' encrusted polymeric nanoparticle improves BBB penetration and anticancer activity of doxorubicin. *Int. J. Pharm.* **555**, 77–99. 10.1016/j.ijpharm.2018.11.035 (2019).
9. Sahoo, S. K. & Labhasetwar, V. Nanotech approaches to drug delivery and imaging. *Drug Discov Today*. **8** (24), 1112–1120. 10.1016/S1359-6446(03)02903-9 (2003).
10. Danhier, F. et al. PLGA-based nanoparticles: An overview of biomedical applications. *J. Controlled Release*. **161** (2), 505–522. 10.1016/j.jconrel.2012.01.043 (2012).
11. Yang, B., Dong, Y., Wang, F. & Zhang, Y. Nanoformulations to Enhance the Bioavailability and Physiological Functions of Polyphenols. *Molecules* **25** (20), 4613. 10.3390/molecules25204613 (2020).
12. Danaei, M. et al. Impact of Particle Size and Polydispersity Index on the Clinical Applications of Lipidic Nanocarrier Systems. *Pharmaceutics* **10** (2), 57. 10.3390/pharmaceutics10020057 (2018).
13. Yang, X. et al. Anti-cancer effects of nitazoxanide in epithelial ovarian cancer in-vitro and in-vivo. *Chem. Biol. Interact.* **400**, 111176. 10.1016/j.cbi.2024.111176 (2024).

14. Abd El-Fadeal, N. M., Nafie, M. S. & El-kherbetawy, K. Antitumor Activity of Nitazoxanide against Colon Cancers: Molecular Docking and Experimental Studies Based on Wnt/β-Catenin Signaling Inhibition. *Int. J. Mol. Sci.* **22** (10), 5213. 10.3390/ijms22105213 (2021).
15. Di Santo, N. & Ehrisman, J. A functional perspective of nitazoxanide as a potential anticancer drug. *Mutat. Res. - Fundamental Mol. Mech. Mutagen.* **768**, 16–21. 10.1016/j.mrfmmm.2014.05.005 (2014).
16. Lü, Z. et al. Nitazoxanide and related thiazolides induce cell death in cancer cells by targeting the 20S proteasome with novel binding modes. *Biochem. Pharmacol.* **197**, 114913. 10.1016/j.bcp.2022.114913 (2022).
17. Ripani, P. et al. Thiazolides promote G1 cell cycle arrest in colorectal cancer cells by targeting the mitochondrial respiratory chain. *Oncogene* **39** (11), 2345–2357. 10.1038/s41388-019-1142-6 (2020).
18. Ghosh, C. et al. Combination nitazoxanide and auranofin treatment has synergistic anticancer activity in anaplastic thyroid cancer through enhanced activation of oxidative stress that leads to apoptosis. *Cancer Lett.* **633**, 217990. 10.1016/j.canlet.2025.217990 (2025).
19. Senkowski, W. et al. Three-Dimensional Cell Culture-Based Screening Identifies the Anthelmintic Drug Nitazoxanide as a Candidate for Treatment of Colorectal Cancer. *Mol. Cancer Ther.* **14** (6), 1504–1516. 10.1158/1535-7163.MCT-14-0792 (2015).
20. Lu, X. et al. CTEN Inhibits Tumor Angiogenesis and Growth by Targeting VEGFA Through Down-Regulation of β-Catenin in Breast Cancer. *Technol. Cancer Res. Treat.* **20** 10.1177/15330338211045506 (2021).
21. Wang, K., Qiu, X., Zhao, Y., Wang, H. & Chen, L. The Wnt/β-catenin signaling pathway in the tumor microenvironment of hepatocellular carcinoma. *Cancer Biol. Med.* **18**, 0–0. 10.20892/j.issn.2095-3941.2021.0306 (2021).
22. Morita, M. et al. Role of β-Catenin Activation in the Tumor Immune Microenvironment and Immunotherapy of Hepatocellular Carcinoma. *Cancers (Basel)*. **15** (8), 2311. 10.3390/cancers15082311 (2023).

Figures

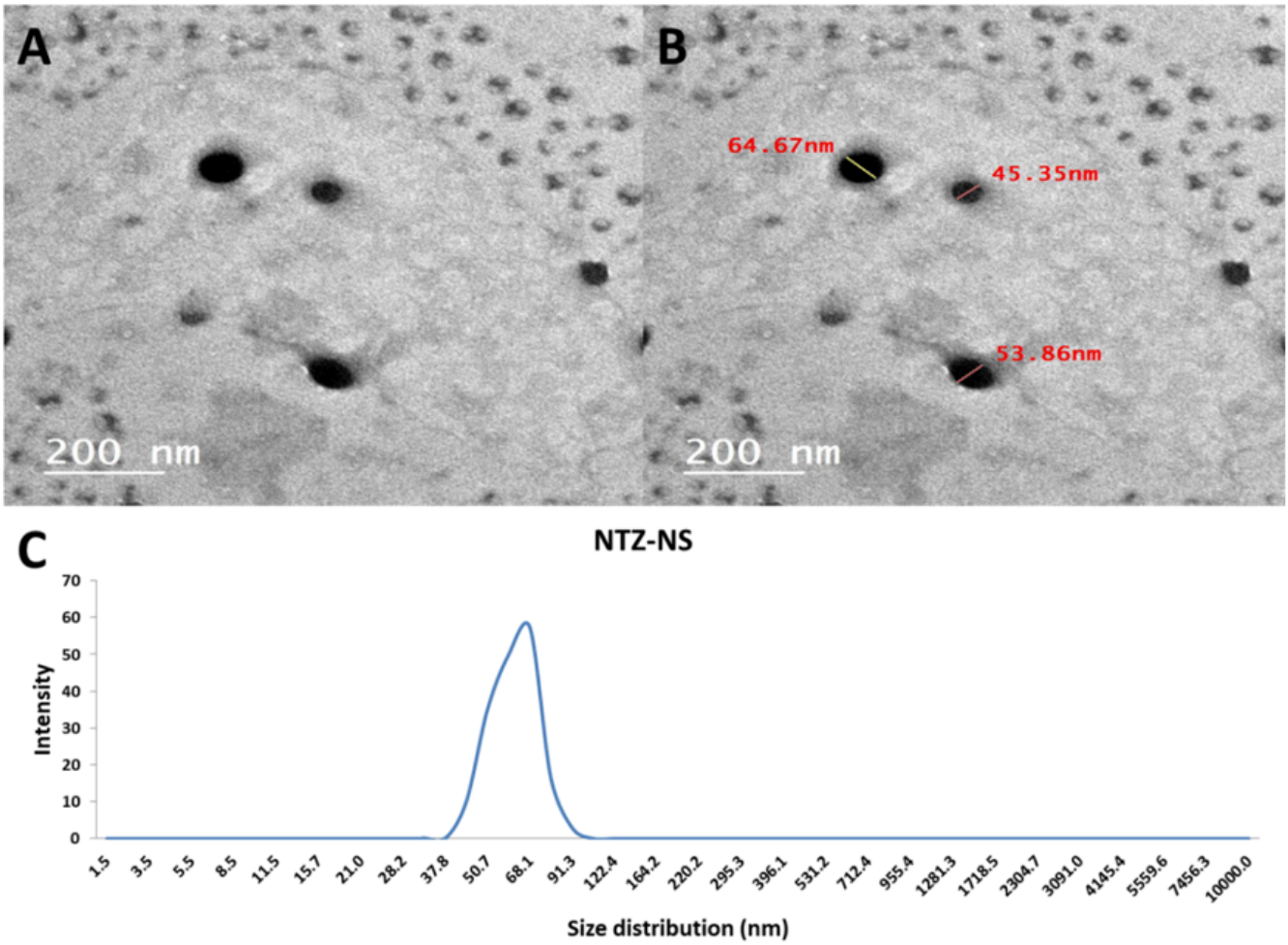

Figure 1

Morphological and size characterization of nitazoxanide nanoparticles (NTZ-NS).
(A and B) TEM micrographs showing spherical, well-dispersed NTZ nanoparticles with diameters of 64.67 nm, 45.35 nm, and 53.86 nm. (C) DLS size distribution profile confirming a hydrodynamic diameter consistent with TEM measurements, indicating uniform nanoparticle size and stable dispersion

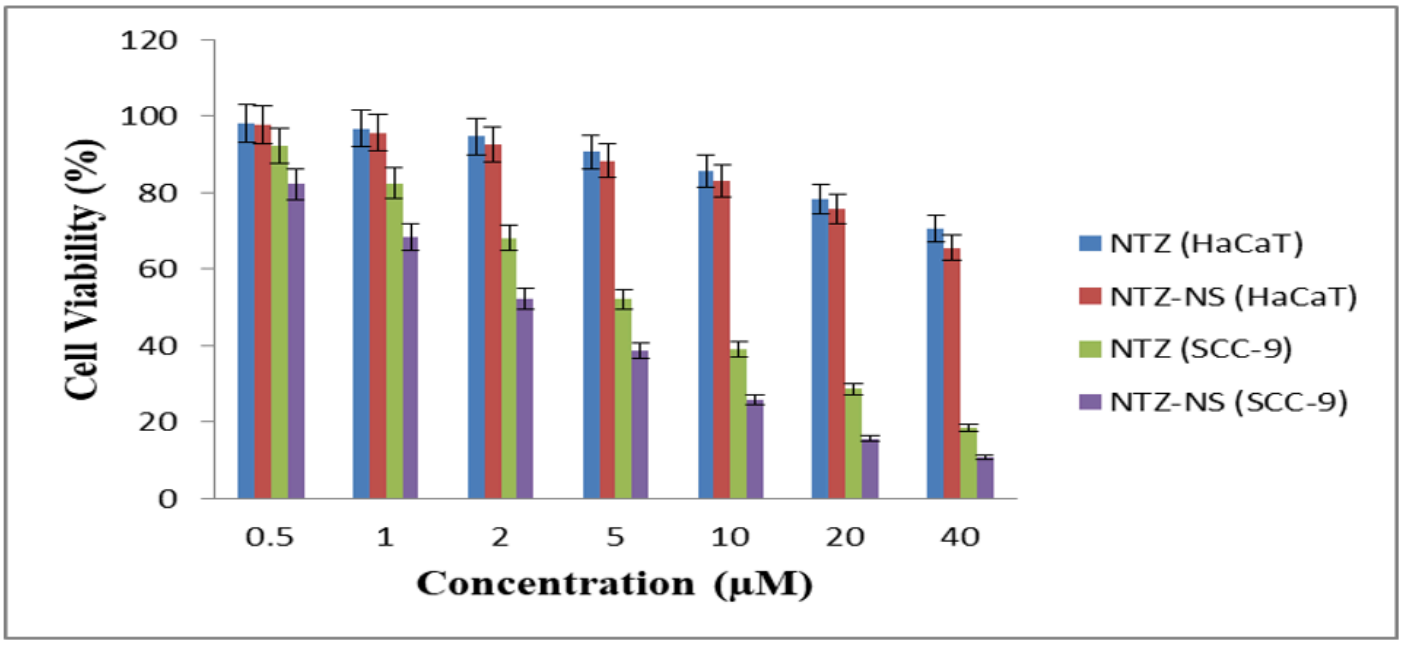

Figure 2

Dose-dependent cytotoxic effects of NTZ and NTZ-NS on SCC-9 and HaCaT cells. Cells were treated for 24 h with seven concentrations (0.5–40 µM) and cell viability was assessed by MTT assay. Free NTZ decreased SCC-9 viability in a concentration-dependent manner, while NTZ-NS exhibited enhanced cytotoxicity at lower concentrations. HaCaT cells showed minimal viability reduction, demonstrating selectivity. IC_{50} values for SCC-9 cells were calculated as ~2.1 µM for NTZ and ~1.5 µM for NTZ-NS. Data represent mean ± SD of three independent experiments

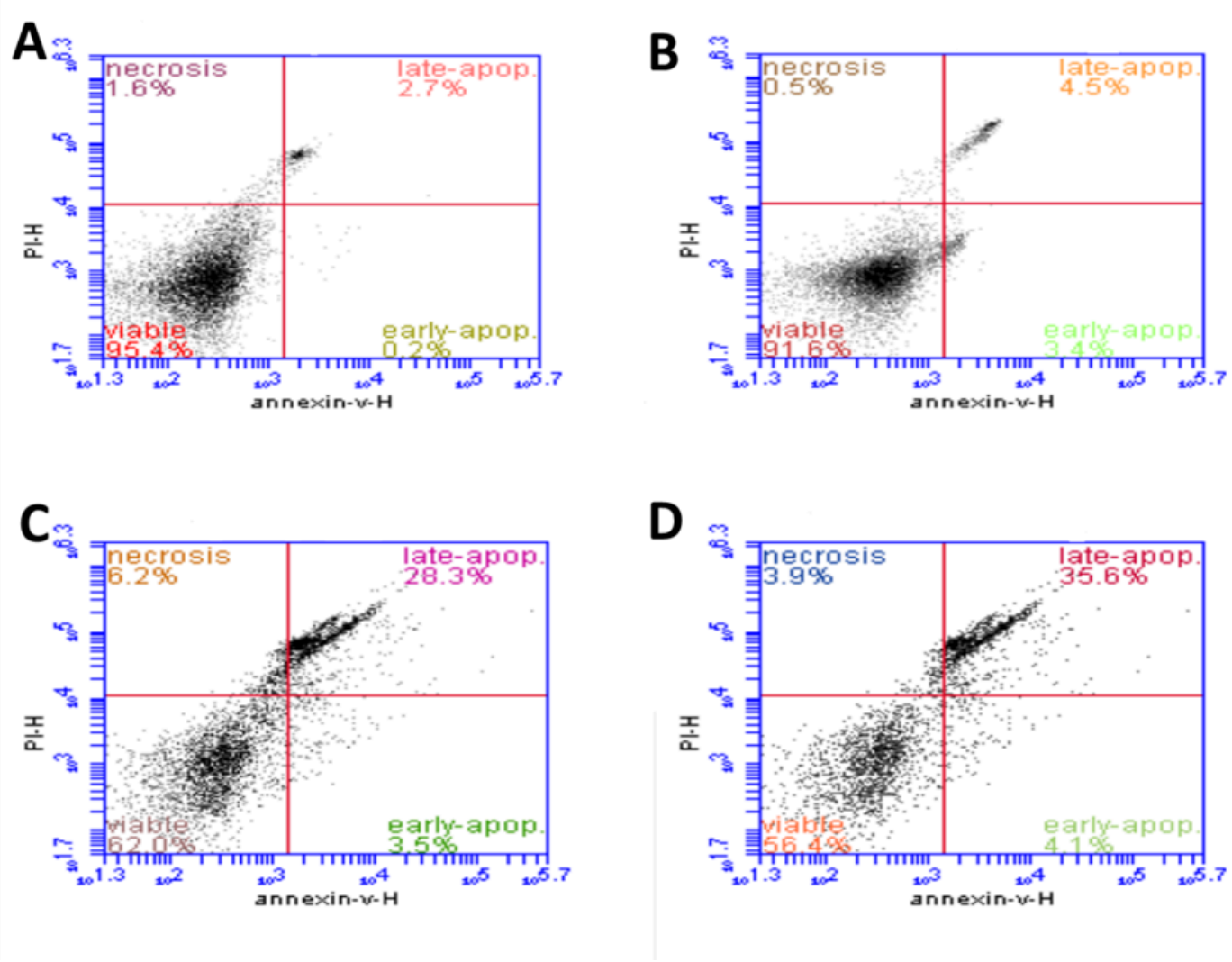

Figure 3

Flow cytometric analysis of apoptosis in HaCaT and SCC-9 cells following treatment with NTZ and NTZ-NS for 24 h. (A) HaCaT cells (negative control), (B) SCC-9 cells (positive control), (C) SCC-9 cells treated with free NTZ, and (D) SCC-9 cells treated with NTZ-NS. Data are expressed as percentage of viable, early apoptotic, late apoptotic, and necrotic cells. Nanoformulation significantly enhanced late apoptosis and necrosis compared to free NTZ

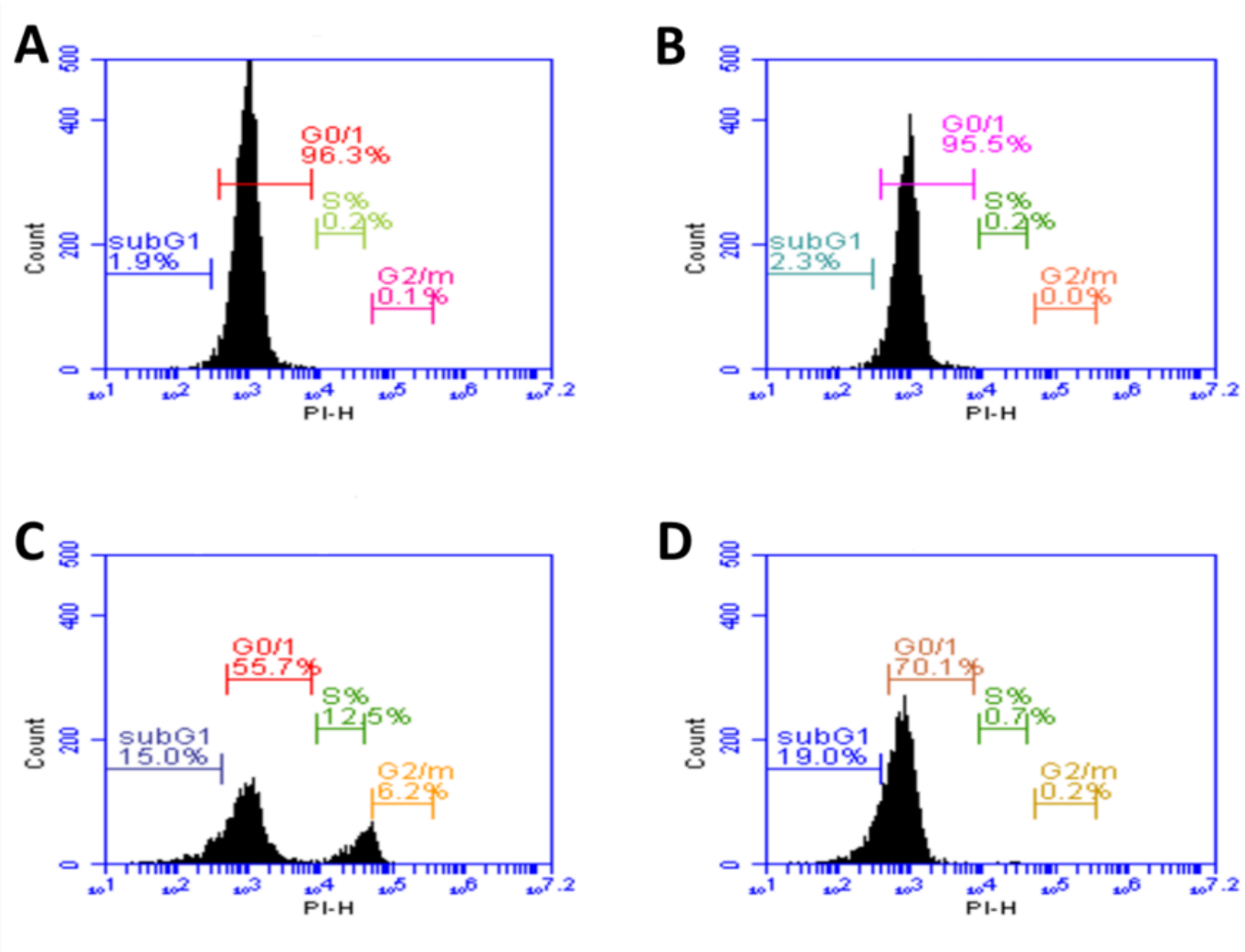

Figure 4

Cell-cycle distribution of HaCaT and SCC-9 cells following treatment with NTZ and NTZ-NS for 24 h, analyzed by flow cytometry. (A) HaCaT cells (negative control), (B) SCC-9 cells (positive control), (C) SCC-9 cells treated with free NTZ, (D) SCC-9 cells treated with NTZ-NS. Data are presented as percentage of cells in subG1, G0/G1, S, and G2/M phases. NTZ-NS induced the highest subG1 accumulation and effectively disrupted cell-cycle progression compared to free NTZ

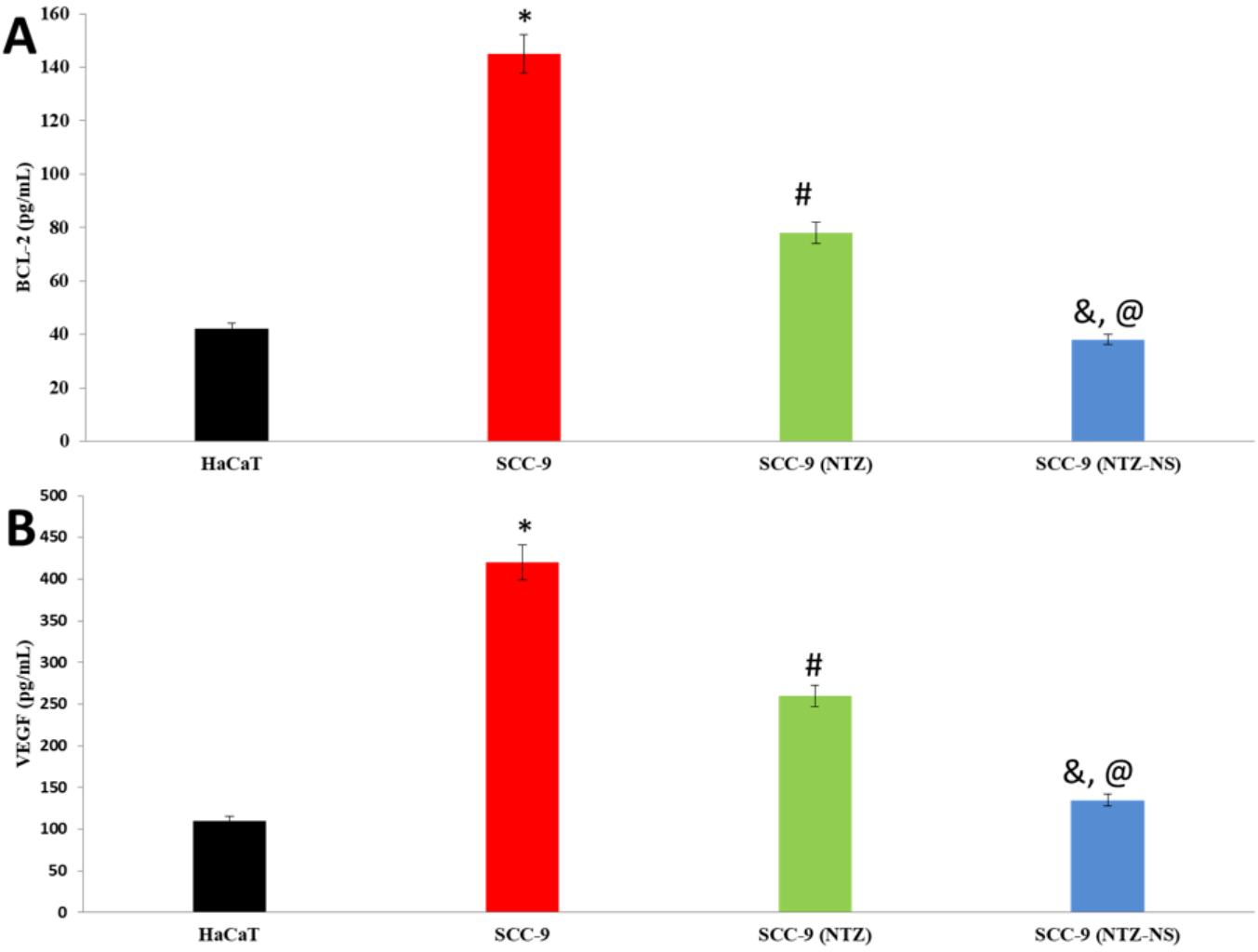

Figure 5

Effect of NTZ and NTZ-NS on biomarkers in SCC-9 cells. Quantitative ELISA analysis of BCL-2 and VEGF levels in HaCaT normal keratinocytes (negative control), SCC-9 oral squamous carcinoma cells (positive control), SCC-9 treated with free NTZ, and SCC-9 treated with NTZ-NS. NTZ-NS induced significantly greater downregulation of BCL-2 and VEGF compared to free NTZ, indicating enhanced pro-apoptotic and anti-angiogenic activity. Data are presented as mean ± SD. *: significant difference between HaCaT and SCC-9 ($p<0.05$), #: significant difference between SCC-9 (NTZ) and SCC-9 ($p<0.01$), and &: significant difference between SCC-9 (NTZ-NS) and SCC-9 ($p<0.01$), @: significant differences between SCC-9 (NTZ) and SCC-9 (NTZ-NS) ($p<0.05$)